ORIGINAL ARTICLE

A stationary shoulder with fluid temperature control for friction stir welding of polymers: development and investigation

Erhard Buchmann[1] · Michael Erdmann[1] · Mathias Köberl[2] · Philipp Höfer[1]

Abstract

There is a growing interest in the application of thermoplastics and thermoplastic composites for lightweight structures, thus also in friction stir welding (FSW) as a suitable joining technology. With the transformation of FSW from metals to polymers, several new tooling concepts were developed; mainly various heating setups to add external thermal energy to the process were designed. However, current temperature control approaches do not consider the cooling of the process at high rotational speeds and the asymmetry of the process in thermomechanical conditions. In this paper, we present a stationary shoulder with fluid temperature control, which is also capable of cooling the process. Additionally, asymmetric temperature control conditions can be examined by applying different flow directions. For investigation, butt welds of PMMA sheets were welded and assessed using the weld morphology and tensile strengths. Different fluid temperatures, feed rates, and both flow directions were applied and led to different tensile strengths. It could be shown that the optimal control temperature is different for the advancing side (AS) and the retreating side (RS). By using a transverse flow, a heat transport from the warmer AS to the colder RS could be established, which improved the strength. Moreover, the tensile strength could be increased by cooling the process at a feed rate of 100 mm/min. To improve the effectiveness of the temperature control, a new shoulder with independent temperature-controlled areas is proposed.

Keywords Friction stir welding (FSW) · Polymer · Thermoplastic · Stationary shoulder · PMMA · Temperature control

1 Introduction

High-performance lightweight structures currently consist mainly of metal alloys and fiber-reinforced plastics with a thermoset polymer matrix. Recently, high-performance thermoplastics are moving more into focus because of better recyclability and lower costs. Accordingly, there is growing industrial demand for suitable joining methods. Welding methods, in particular friction stir welding (FSW), are beneficial regarding stiffness and strength. Additional advantages of FSW include energy efficiency, the applicability to many materials, and the possibility of welding dissimilar materials [1]. This makes the FSW process especially suitable for high-performance lightweight structures.

The FSW process is based on the generation of frictional heat and the material transport through a rotating tool. Specifically, a non-consumable rotating pin is pressed through adjacent joining partners, as shown in Fig. 1. The joining partners are kept in place through the clamps and the backing plate. They are heated up through the frictional heat caused by the rotation of the pin and the pressure generated through the feed motion. Thus, the material becomes less viscous in the stir zone and is extruded around the pin [2]. Behind the pin, the transported material forms the weld seam and generates a bond between the joining partners as it consolidates. A shoulder concentric to the rotating pin is led over the joining partners. Rotating and non-rotating

✉ Erhard Buchmann
  erhard.buchmann@unibw.de

  Michael Erdmann
  michael.erdmann@unibw.de

  Mathias Köberl
  mathias.koeberl@unibw.de

  Philipp Höfer
  philipp.hoefer@unibw.de

[1] Institute of Lightweight Engineering, Universität der Bundeswehr München, Werner-Heisenberg-Weg 39, Neubiberg 85577, Germany

[2] Institute for Construction Materials, Universität der Bundeswehr München, Werner-Heisenberg-Weg 39, Neubiberg 85577, Germany
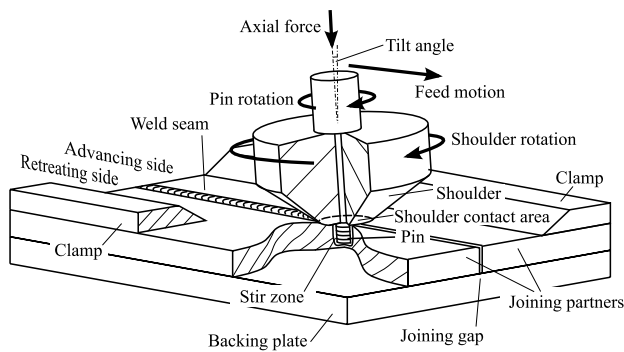
Fig. 1 Scheme of the friction stir welding process

(stationary) shoulders are distinguished: When the shoulder rotates and is pressed on the joining partners with an axial force, additional frictional heat is transferred into the material. Moreover, the shoulder rotation influences the material transport conditions. When the shoulder is stationary, it serves as a constraint for the viscous material in the stir zone.

Already with the invention of FSW in 1991, the process was patented for metals and thermoplastics [3]. While the process is well established for metals, especially aluminum alloys [4], it is still the subject of current research for polymers and polymer composites [5–8]. When using thermoplastics as base material for friction stir welding, a number of essential differences in the thermomechanical and rheological properties compared to metals must be considered (cf. [5]):

- Polymers have a relatively low melting temperature compared to metals [9].
- Polymers feature a lower thermal conductivity than metals. For instance, the thermal conductivity of aluminum ($228 \frac{J}{msK}$) is 456 times higher than the one of polyethylene ($0.5 \frac{J}{msK}$) [9].
- The rheological behavior differs from that of metals. Notably, the viscosity of polymers lowers with higher shear rates and higher temperatures. There is a substantial change in viscosity when reaching the glass transition temperature. This behavior is further influenced by crystallinity [9, 10].
- The friction coefficients between the pin, which usually is metal, and the base material strongly depend on the polymer type used. For instance, the friction coefficient of polyamide and steel (0.35) is almost twice as high as the one of polyethylene and steel (0.2) [9].
- The stiffness of the base material is reduced significantly when reaching the glass transition temperature. This must be considered when controlling the axial force on the shoulder [9].
- The thermoplastic base material is melted during friction stir welding, while it is only softened when welding aluminum [11].

The research work on FSW of polymers is reviewed in [5–8]. It can be organized using three foci: welding tool, process configuration, and process parameters, which is depicted in Table 1 (cf. [12]). However, fundamental advances in FSW for polymers could be achieved using new welding tools and new process configurations instead of transferring them from the metal FSW process and optimizing process parameters only. In particular, the process can be improved by making two major adaptions to the welding tool (cf. [11, 13]):

- Using a stationary shoulder
- Applying an additional process temperature control

Both adaptions are considered in this study. A key contribution therein is the development of the *Hot Shoe* welding tool: a stationary shoulder equipped with an external heat source [11]. Up to now, several more temperature control approaches for the FSW process have been developed. This includes heating the shoulder and the pin via the friction of the probe with the shoulder [14, 15], via an induction loop [16], via an integrated heating element [17] and heating the base material [18]. However, the process still lacks high strengths and has only low feed rates. This makes the process inappropriate for industrial needs.

Table 1 Influence of variables on the FSW process besides the mechanical and thermal properties of the base material (cf. [12])

Welding tool	Process configuration	Process parameters
• Pin geometry: diameter, length, contour • Shoulder geometry: type of shoulder (rotating/stationary), diameter, contour • Pin and shoulder materials • Thread pitch • Temperature control of the tool	• Joint configuration (e.g. butt joint, lap joint) • Characteristics of FSW process phases • Axial position control (force-controlled or position-controlled) • Clamping setup • Thermal boundary conditions, esp. of the backing plate • Further heating facilities (e.g., radiation heating) • Further control strategy (e.g., feedrate, rotation speed)	• Rotation speed • Tool traverse speed • Tilt angle • Tool rotation directions • Plunge force or depth

A major challenge is that high feed rates lead to poor material mixing. The material mixing can be improved with higher rotational speeds, which cause higher welding temperatures simultaneously. But, too high rotational speeds lead to poorer strengths and are limited to a maximum when degradation of the base material begins. Due to this coupling, feed rates are currently also limited. However, cooling the process at high feed rates and high rotational speeds was not considered until now.

Moreover, the process is asymmetric regarding the thermomechanical and flow conditions in the stir zone: On the advancing side (AS), the feed motion and the motion of the pin surface are in the same direction, whereas the two motions are in the opposite direction on the retreating side (RS). This leads to different bonding strengths on both sides. Nonetheless, this is not taken into account for the temperature control concepts because AS and RS were always heated equally until now.

Simões et al. [13] investigated FSW for a 10-mm-thick polymethylmethacrylate (PMMA) plate with a rotational tool. They report significant differences in the weld morphology of RS and AS, whereas the retreating side could be identified as the preferential location for defect formation. The authors claim that these defects on the RS are "one of the main weldability problems for polymers." They suppose that those discontinuities can be avoided by welding at lower temperatures. However, no cooling system was investigated. The investigated pins were only 5 mm and 6 mm long resulting in bead on plate welding only. Accordingly, the influence of the backing plate and the fixture was neglected. Nonetheless, it was not researched how the remaining 5-mm or 4-mm thickness of the PMMA plate could be replaced when performing weld seams instead of bead on plate welding.

In the works of Derazkola et al. [19, 20], FSW of polymers is examined using thermomechanical simulations. They report a strong influence of the rotational velocity and transverse speed on the heat fluxes, which influences the quality of the welds. Moreover, a stronger heat generation at the AS than on the RS is reported. However, the influences of the backing plate and the fixture are not investigated. This heat concentration on the AS is also shown in the work of Elyasi et al. [21]. Here T-joints are investigated, and accordingly, no backing plate is used in this study. Eslami et al. [22] examined the influence of the material of the stationary shoulder on FSW of polymers by applying a wood, teflon, aluminum, polycarbonate, and brass shoulder with a metal backing plate. They report that the process heat accumulates in the brass shoulder instead of staying in the process. Consequently, a teflon shoulder with friction heating is applied. However, the influence of the material used for the clamping and the backing plate is not considered. They furthermore report a lack of good stirring and heat generation on the RS. Derazkola et al. [19] could show in simulations that the resulting temperature gradient can be reduced with higher rotational speeds. Moreover, they claim a different material flow on both sides due to different strain rates resulting in different viscosities. Nonetheless, no external temperature control for homogenizing of the temperature conditions on AS and RS is considered in [13, 19, 21]

Adibeig et al. [23] investigated the FSW process on butt weld joints. They report limits of the rotational speed: A too low rotational speed results in an insufficient material flow, whereas a too high rotational speed leads to the degradation of the base material. Moreover, they report a strong dependence on rotational and traverse speed parameters. They propose a heat index formula to calculate the ideal parameter combination. However, they do not investigate how this coupling could be overcome using an external temperature control that is also capable of cooling the process. Moreover, the thermal influence of the fixture of the joining partners is not considered.

Nelson et al. [11] presented the *Hot Shoe*, a stationary shoulder equipped with an external heat source. Cooling air is used to maintain a constant shoulder temperature. Moreover, they mention that the heat generated by too high rotational speeds (higher than 1400 rpm) leads to degeneration of the base material. Despite investigating the influence of introducing thermal energy through the shoulder, the heat loss through the fixture is not considered. In Mendes et al. [24], the concept of a *Hot Shoe* is integrated with a force-controlled robotic welding system with a metal backing plate. It is outlined that due to the high thermal inertia and the fact that the tool is only heated and not cooled, it overheats in some cases. In Moochani et al. [25], a heat gun combined with a temperature sensor is used to heat the stationary shoulder and the pin and maintain a specific temperature. The authors found that a higher rotational speed leads to better mixing. In another study [26], a *Hot Shoe* with a closed-loop temperature controller is used for FSW of PMMA sheets. The authors claim that high rotational speeds lead to higher tensile strengths due to better material mixing, but spindle speeds higher than 1600 rpm lead to poorer welding beads due to localized melting. Moreover, they report that high feed rates lead to poor mixing. Bagheri et al. [27] took Nelson's *Hot Shoe* to investigate FSW of ABS sheets. An electrical thermal element heats the stationary shoulder that is set right onto the joining partners. It is reported that all tensile specimens broke on the RS. The authors claim that the temperature on the AS is higher than that on the RS and that high feed rates lead to poor material mixing. Nevertheless, an asymmetric temperature control was not considered here. These studies on FSW of polymers [11, 24–27] commonly report the degradation of the welding partners at high rotational speeds and the asymmetric temperature conditions of the process. Moreover, the thermal influence of the fixture is generally not addressed. However, a temperature control that can effectively maintain

a constant shoulder temperature or even cool the process at high rotational speeds is not considered.

In this work, a new welding tool with a fluid temperature control that is capable of heating and cooling the FSW process is developed and investigated using PMMA. By using a transverse water flow, asymmetric temperature control conditions on AS and RS could be examined. For the backing plate, PEEK (polyether ether ketone) is used. In doing this, the heat flux out of the process into the backing plate could be reduced to a minimum which allows effectively steering the process temperature through the cooling fluid.

2 Method

A new welding tool with a fluid temperature control was developed and used to produce butt welds using a conventional position-controlled milling machine. The joints were assessed using the tensile strengths, the morphology of the cross section, the morphology of the fracture surfaces, and the microstructure before and after welding.

2.1 Materials

Extruded PMMA sheets were used as a base material. This polymer is amorphous and allows an easy optical evaluation of the joint quality due to its transparency. It has a rather low glass transition temperature of 112 °C, which was determined using a thermomechanical analysis (TMA). The strength of the base material is 57 MPa with a standard deviation of 2.4 MPa.

2.2 Experimental procedure

Two PMMA plates of 4.9 mm × 300 mm × 95 mm were clamped alongside the joint direction to produce butt welds. A polished PEEK plate of 10-mm thickness was used as a backing plate (see Fig. 3). By doing this, the heat flux out of the welding region into the backing plate could be reduced
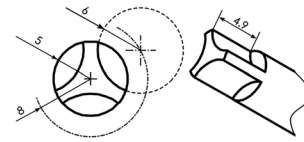

Fig. 2 Pin geometry with three flutes

due to the low thermal conductivity of PEEK. The joining partners were clamped on the PEEK plate with two clamping claws on each side. In order to prevent too high surface pressure of the clamping claws on the PMMA plates, additional steel plates were used as washers. An axial force of 400 N and a tilt angle of 0° was used.

The main FSW process parameters are summarized in Table 2. This study used a constant high rotational speed of 2000 rpm to provide good material mixing. The effect of the new temperature control approach was tested with three different very high feed rates of 50, 100, and 150 mm/min.

Most relevantly, the control temperature inside the shoulder was varied. To define a benchmark, the joints were made without temperature control first. Doing this, the shoulder was empty and heated passively by the welding process. Then, the same joints were produced using a water temperature of 20 °C and 60 °C with a volumetric flow rate of approx. $2.3 \cdot 10^{-5} \frac{m^3}{s}$. At both temperatures, both possible flow directions were tested.

2.3 Pin geometry

An overview of pins used for friction stir welding of polymers can be found in [5, 6], and [11]. However, there is no uniform recommendation for the pin geometry. Consequently, in this study, a pin based on the Triflute™ and the Flared-Triflute™ was used as they are very successful in FSW of metals [1, 28] which is depicted in Fig. 2. Furthermore, to reduce additional axial forces, the pin is not tapered.

Table 2 Main FSW process parameters

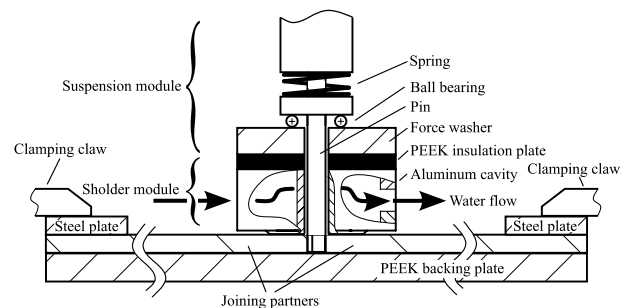| Parameter	Value	Unit
Rotational speed	2000	rpm
Feed rates	50, 100, 150	mm/min
Tilt angle	0	°
	No temperature control	-
Temperature control approach	20	°C
	60	°C
Flow directions	AS to RS	-
	RS to AS	-

Fig. 3 Functional structure outline of the developed tool with suspension module and shoulder module in a sectional view perpendicular to the welding direction. The joining partners are clamped on a PEEK backing plate with clamping claws and steel plates during FSW
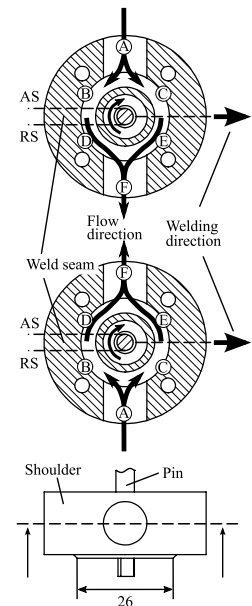
Fig. 4 Detailed description of the stationary shoulder with a temperature control and axially elastic mounting. The components of its suspension and shoulder module are depicted in (**a**) and described in (**b**). The flow from the advancing side (AS) to the retreating side (RS) and the reverse flow of the cooling water are visualized in (**c**). The flow begins at the inlet (A), continues with one stream behind the pin (B, D) and one stream at the front of the pin (C, E), and leaves the shoulder at the outlet (F)
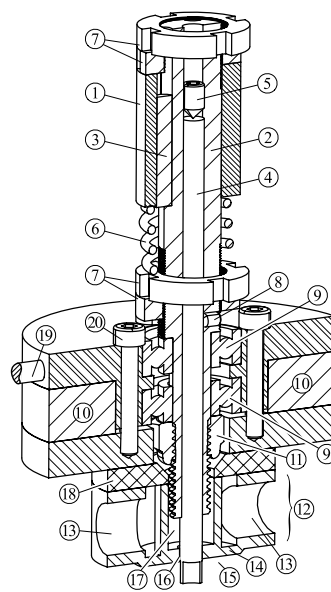
Module	Nr.	Component
Suspension module	1	Hull with clamping surface
	2	Central shaft
	3	Dowel pin for shaft-hub connection
	4	Pin
	5	Plunge depth adjustment screw
	6	Spring
	7	Shaft nuts
	8	Grub screw
	9	Ball bearing
	10	Force washer
	11	Clamping nut
Shoulder module	12	Aluminum cavity
	13	Water inlet/outlet
	14	Heat conduction plate
	15	Shoulder contact area
	16	Pin shoulder gap
	17	Trap cavity for material escaping through the pin shoulder gap
	18	PEEK insulation plate
	19	Bracket to keep the shoulder stationary
	20	Clamp screw for force washer pre-tension

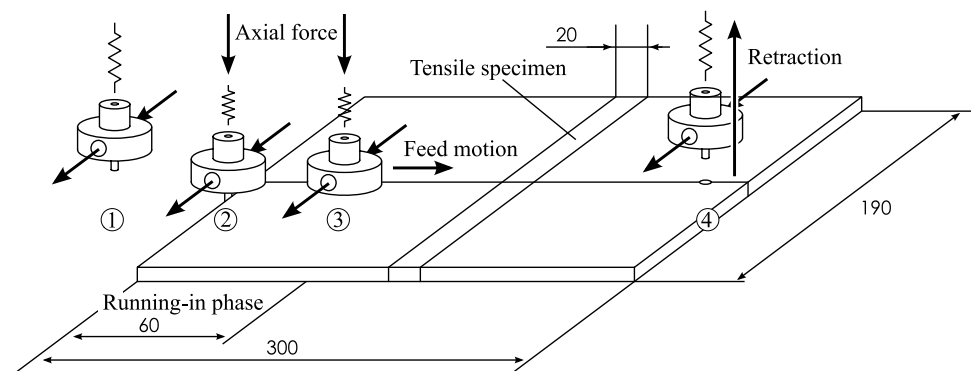(**a**) Sectional drawing   (**b**) Components of the modules   (**c**) Visualization of the flow in the aluminum cavity

2.4 Tensile testing and weld seam analysis

The quality of the weld beads was assessed by investigating the optical appearance and evaluating the tensile strengths based on [29]. Tensile specimens were cut out of the PMMA sheets after the running-in phase (see Fig. 5). For comparison purposes, the same tensile specimen geometry (190 mm × 20 mm × 4.9 mm) was used for testing the base material. The tensile strengths of five specimens were measured on a universal testing machine (Zwick Z150). The mean and the standard deviation were calculated. Moreover, it was observed if the specimens broke on the AS or RS. The fracture surfaces were analyzed optically using a PCE-MM 200 microscope. For the investigation of the microstructure, a Fourier transform infrared spectrometer with attenuated total reflectance (ATR) attachment (Thermo Fisher Scientific Nicolet iS10) in the wave number range of 600–4000 cm^{-1} was applied.

3 Results and discussion

3.1 Stationary shoulder with fluid temperature control and axially elastic mounting

A stationary shoulder with a fluid temperature control and axially elastic mounting was developed. The functional structure is depicted in Fig. 3, whereas a detailed description can be found in Fig. 4. The shoulder can be divided into two modules:

- Suspension module
- Shoulder module

The suspension module serves as a mount for the shoulder module and rotates the pin. It is axially elastic and equipped with a force measurement. By doing this, it is easy to adjust the vertical force on the process, although a stiff

Fig. 5 Phases of the experimental welding procedure: (**1**) establishing the cooling water flow, (**2**) setting the axial force, (**3**) welding, (**4**) retraction. The tensile specimens were cut out after the running-in phase, in which the FSW process consolidates after plunging in laterally

position-controlled conventional milling machine is used for friction stir welding in this work. Furthermore, small irregularities in the thickness of the base material can be tolerated easily. Notably, the stationary shoulder will always be pressed on the base material preventing stirred material from escaping. As the contact pressure is relatively constant, reproducible thermal transfer conditions are realized.

The shoulder module is equipped with a cavity for the transverse water flow. Using water as a heat transfer fluid allows a high heat transfer and the use of a customary boiler. A PEEK plate serves as insulation of the shoulder module from the suspension module. Thus, the heat transfer between the shoulder module and the mounting module is kept on minimal level. Through the very high volumetric flow and the excellent insulation of the PEEK backing plate and the PEEK insulation plate, the process temperature can be influenced very effectively by the cooling water. Notably, it is possible to vary the shoulder temperature independently from the process and to keep it at the adjusted value, also below the process temperature. The transversal flow allows the investigation of different heating conditions on the AS and RS when changing the flow direction. In the following, both modules are described in detail.

The suspension module is clamped into a standard milling machine with the clamping surface of the hull (1). The central shaft (2) can move axially relative to the hull, creating an axial force through the spring (6). It rotates the pin (4) and holds its axial and lateral position. Shaft nuts (7) serve to adjust the spring hardness. The lateral and axial forces of the shoulder are transferred into the milling machine with the bearing (9). The suspension module is made of steel because of its high stiffness and hardness. In contrast to that, aluminum was chosen for the shoulder module owing to its good heat conduction.

The shoulder module is mounted onto the suspension module via a preloaded ball bearing support in an O-arrangement (9,11) that transfers the forces and allows the relative rotation between the shoulder and the suspension module. It is kept in place (stationary) by a bracket (19) connected to the milling machine. The axial forces on the shoulder are measured by the force washer (KISTLER Type 9071, 10) to guarantee a constant contact pressure of the shoulder contact area (15). The fluid flows transversely to the feed motion through the aluminum cavity (12) through the water inlets/outlets (13) (see Fig. 4c). The direction of the water flow through the stationary shoulder can be reversed. Thus, different temperature control conditions on the AS and RS are enabled. The aluminum cavity is insulated from the upper parts by the PEEK plate (18). A pin shoulder gap (16) of 0.1 mm was selected, which guarantees a frictionless pin rotation and reduces the material escaping from the stir zone. The thin (2 mm) heat conduction plate (14) ensures an effective heat transmission from the cooling water to the surface of the welding partners. The shoulder contact area is not contoured.

3.2 Preliminary experiments

Preliminary tests showed that a poor quality of the joining surfaces and a large joining gap result in a weld bead with many defects. Therefore, the adjacent joining surfaces were milled to get a smooth and even surface and are clamped directly onto each other.

When plunging axially into the base material, viscous material is extracted onto the surface of the joining partners around the pin. This hinders the complete contact of the shoulder contact area with the base material. Furthermore, this allows material to escape when advancing the tool and impairs the heat transfer from the shoulder to the welding partners. Therefore, the tool is plunged into the base material from the edge with lateral force (see Fig. 5). Hence, the following procedure was applied to weld the PMMA sheets (see Fig. 5): First, the cooling water flow was established (1). This phase is not applied when welding without temperature control. Secondly, the shoulder is pressed onto the base material with an axial force of 400 N and a tilt angle of 0° (2). In doing so, the spring of the suspension module is compressed. Then, the pin is pressed laterally into the joining gap with a pin plunge depth of 4.8 mm. Third, the tool is led over the joining partners while welding (3). When entering the base material from the edge, the stirred material is expelled laterally. This leads to defects in the weld seam initially, but the process stabilizes when the tool moves forward. After the running-in phase of 60 mm, there is a constant FSW process. Finally, the tool is retracted (4).

3.3 Overview over results

The influence of the parameters feed rate, control temperature, and flow direction on the tensile strength is depicted in Fig. 6. The most significant influence on the tensile strength is the feed rate: The higher the feed rate, the lower the measured tensile strength. Notably, the tensile strength of a specimen welded at 150 mm/min using no temperature control is only approximately 30% of the one welded at 50 mm/min. On the other hand, the highest tensile strength of 50% of the base material's tensile strength could be achieved with a feed rate of 50 mm/min and two temperature control configurations: no temperature control or a control temperature of 60 °C with flow from the AS to the RS ($A \rightarrow R$). Moreover, the tensile strength is remarkably influenced by the temperature control regime. The structure of the fracture surface decidedly depends on the feed rate (see Fig. 9). It is assumed that this shoulder effectively hinders the thermal degradation of PMMA which was deduced from the microstructure analysis. The results are analyzed in detail in the following.
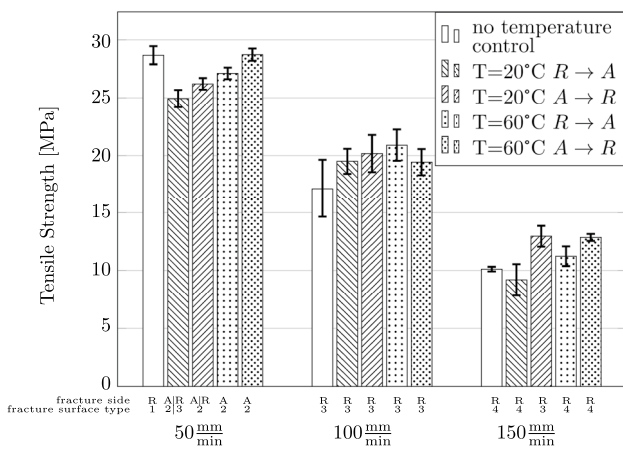
Fig. 6 Mean tensile strength (5 specimens) and standard deviation for the feed rates 50 mm/min, 100 mm/min, and 150 mm/min using a rotational speed of 2000 rpm. The tensile specimens broke either all on the retreating side (R), all on the advancing side (A), or not uniformly on one side (A|R). The shoulder can be empty (no temperature control) or a flow of cooling water of 20 °C or 60 °C is established. Two flow directions were used: The current enters the shoulder on the retreating side, flows around the pin, and exits the shoulder on the advancing side ($R \rightarrow A$) or is reversed ($A \rightarrow R$). Four different types of fracture surfaces (1,2,3,4) were identified (see Fig. 9)

3.4 Analysis of the welded joints at a feed rate of 50 mm/min

At the feed rate of 50 mm/min, the welded specimens broke on different sides depending on the temperature control regime, as depicted in Fig. 6. Therefore, the corresponding cross sections were investigated. Exemplary cross sections and weld bead surfaces are depicted in Fig. 7. Different zones can be identified from the top view (Fig. 7b) and the cross section under back light (Fig. 7a). The joint consists of one bond on the AS and one bond on the RS with the weld bead in between. The weld bead is transparent in its

cross section but not from the top view (see Fig. 7a) and is minimally wider than the pin. There are bubbles under the surface of the weld bead (see Fig. 7a). It was observed that the number of bubbles increases with higher feed motion. However, a reduction of this number using a temperature control could only be reached at 100 mm/min with a temperature of 20 °C. The specimens always broke at the bonds and never in the weld seam or in the base material. Consequently, it was assumed that the number of bubbles is not crucial for the strength. The bond can be seen clearly on the RS due to irregularities that break the backlight. On the AS, the bond has sparse defects. There, the position of the border between the base material and the weld bead can be seen from the top view (see Fig. 7a) but hardly in the cross section (see Fig. 7b). Moreover, the bond on the RS does not cover the whole thickness of the sheets: At the surface, there is a lack of material between weld bead and base material, which further influences the joint strength. However, the welds welded with 50 mm/min using a control temperature of 60 °C ($A \rightarrow R$) and no temperature control have approximately the same tensile strengths while breaking on different sides. As shown in Fig. 7a, both specimens show a comparable number of irregularities only on the RS. Thus, these defects are not the single reason for the weakness of a bond. One reason could be residual stresses (cf. [13]). Moreover, it can be deduced that this study's approach of an asymmetric temperature control regime on the material flow is not enough to significantly influence the weld morphology.

With the regime "no temperature control", the specimens uniformly broke on the RS, whereas with a control temperature of 60 °C, the specimens uniformly broke on the AS. Consequently, it can be deduced that both sides require different control temperatures to improve their strength. Accordingly, an asymmetric temperature control approach could further improve the process. Furthermore, the specimens welded at 50 mm/min with a temperature control of

Fig. 7 Photo of exemplary cross sections of the weld beads (**a**) and the optical appearance of the surface (**b**)
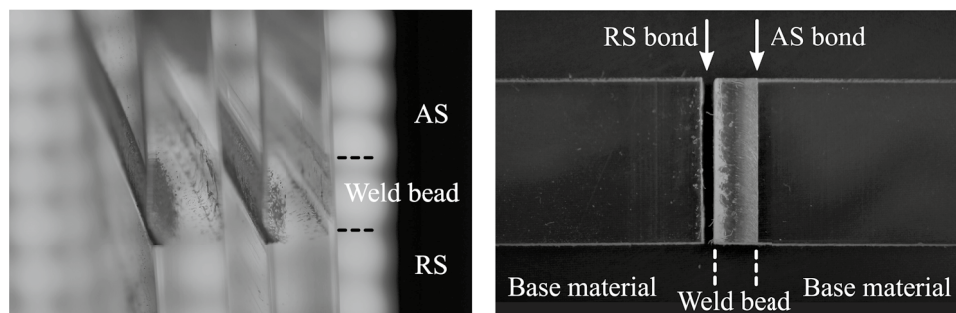
(a) Cross section of weld beads welded with 50 mm/min and 2000 rpm using a control temperature of 60 °C with a flow from the advancing side (AS) to the retreating side (RS) (left) and no temperature control (right).

(b) Broken tensile specimen (broken on the retreating side) welded with 100 mm/min and 2000 rpm using a control temperature of 20 °C with a flow from the advancing side (AS) to the retreating side (RS). The FSW joint consists of the bond on the RS (RS bond), a weld bead and the bond on the AS (AS bond)

20 °C did not break uniformly on one side. So, it is assumed that with a temperature over approx. 20° C, the break side is the AS, whereas with a temperature under approx. 20 °C, the break side is the RS.

Interestingly, no correlation between the flow direction and the break side could be shown in this approach. However, it can be observed that the strength depends on the flow direction. At 50 mm/min and a control temperature of 60 °C, a uniform breakage at the AS with different strengths for both flow directions can be observed. Thus, both flow directions create a better temperature regime for the AS than for the RS. The slight temperature gradient produced by changing the flow direction affects the strength of both bonds. However, it is not enough to generate better strength on either side. It is deduced that there is a considerable gap between the ideal control temperatures for both sides. For this feed rate, 60 °C is nearer to the ideal control temperature for the AS than that for the RS. The temperature control of this work does not allow to set the control temperature for AS and RS independently. For a further evaluation of the ideal control temperature, an approach with two independent heating systems for AS and RS could be used. At 20 °C, a better strength could be reached by applying a flow direction ($A \rightarrow R$) while no uniform break side could be observed. This behavior cannot be explained with the approach of this work. Consequently, the bonding mechanisms of both sides and the correlation to their control temperature should be examined to improve the bonding strength in future work.

The surface of a weld bead shows the typical onion rings of the FSW process, which can be seen in Fig. 7b. There is no expelled stirred material and only minor grooves of the transversal movement of the stationary shoulder (see also Fig. 7a). Hence, the newly designed shoulder effectively seals the stirring zone without requiring an axial force that harms the base material.

3.5 Analysis of the welded joints at feed rates of 100 mm/min and 150 mm/min

All specimens broke uniformly on the RS at the feed rates 100 mm/min and 150 mm/min. Accordingly, the weaker bond is on the RS. Regarding the influence of the temperature control on the RS, the flow direction ($R \rightarrow A$) is considered where the water first reaches the RS. At the other flow direction ($A \rightarrow R$), the water first overflows the AS with a heat exchange at this side, followed by a temperature change. Consequently, the control temperature for the RS is unknown.

Regarding the shoulder contact area (see Fig. 4c), the water preheats or cools the base material in front of the pin, heats or cools the stir zone, and heats or cools the weld bead

behind the pin. In front of the pin, a control temperature of 20 °C has little influence as the experiments were conducted at room temperature, whereas it is a cooling of the process at the stir zone. Namely, during FSW of polymers, the base material is melted [11]. As the glass transition temperature is 112 °C, a control temperature of 60 °C and 20 °C is considered a cooling of the process in the stir zone. When using 20 °C, the tensile strength is improved at 100 mm/min, but lowered at 150 mm/min. It is followed that the strengths can be improved by cooling (20 °C) only at specific feed rates. The process temperature is assumed to be higher at 100 mm/min than at 150 mm/min. Therefore, the strengths can be improved more when using 60 °C. Nevertheless, a control temperature of 60 °C is considered preheating in front of the pin. This approach cannot differentiate between the effect of preheating the base material and cooling the stir zone.

Consequently, the crucial heat fluxes for the strength of the weld are located under the shoulder. In future work, the temperature distribution under the shoulder should be investigated accurately on the one hand. On the other hand, instead of applying a uniform control temperature to the whole shoulder contact area, different zones with independent temperature control should be established (see Fig. 8). The influence of these control temperatures could then be investigated. By doing both, the bonding mechanisms can be better understood. The preheating zone, welding zone, and cooling zone can be distinguished concerning the welding direction. In this course, the advancing and retreating sides should be considered separately. Moreover, the weld bead zone and stir zone temperature should be controlled independently. It is assumed that the stir zone requires cooling at high rotational speeds, whereas the weld bead zone needs to be heated, especially if certain recrystallization is desired.
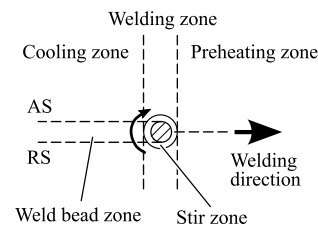

Fig. 8 Proposition of temperature control zones for the shoulder contact area. Instead of applying a uniform control temperature for the whole shoulder, different zones with independent temperature control should be established. In welding direction, the preheating zone, welding zone, and cooling zone can be distinguished. In this course, advancing side and retreating side should be considered independently. Moreover, the temperature of the weld bead zone and stir zone should be controlled separately

3.6　Analysis of the heat transport between advancing and retreating side with the transverse flow

Regarding the water flow at 20 °C, the heat transfer from the process to the cooling water can be examined as the experiments are conducted at room temperature (see Fig. 4c). After entering the shoulder (A), the cooling water first overflows the AS or RS (B, C) and is heated by the process. This heat transfer differs for the two flow directions due to the different AS and RS temperatures. Then the heated water continues to the outlet (F). This course generates a heat transfer between the forming welding bead and the RS or AS (D, E). This heat transfer is higher if the temperature gradient between the AS and RS is more significant. Consequently, the transversal flow balances the process temperature between AS and RS. Accordingly, at a feed rate of 50 mm/min, 100 mm/min, and 150 mm/min, the tensile strength can be improved when applying the flow direction ($A \rightarrow R$) compared to the flow direction ($R \rightarrow A$). The AS (which is considered to be the warmer side [13, 19, 21]) can first heat the water before it overflows the RS. As a control temperature of 60 °C with a flow from the RS ($R \rightarrow A$) generally leads to better tensile strengths, the warmer temperature through the heating of the AS is considered to be the reason for the improved strength. Using the heat of the AS for the RS could make the process more energy-efficient. The flow ($A \rightarrow R$) with 60 °C cannot be investigated in this approach as the process temperature on the AS, and therefore the amount of the heat transfer to the cooling water, is unknown. Interestingly, the effect on the joint strength of the flow direction and the effect of the control temperature on the tensile strength is comparable (Fig. 6).

3.7　Analysis of the fracture surfaces and the microstructure

The optical appearance of all specimens was analyzed using the regions applied in [30]: mirror region, mist region, and hackle region. Based on this investigation, four different types with similar fracture surfaces could be identified (see Fig. 9). The respective fracture surface type of each specimen is depicted in Fig. 6.

Principally, the fracture surface type depends on the feed rate. The characteristic fracture surface type of a specimen welded with a feed rate of 50 mm/min was type 2, for a feed rate of 100 mm/min type 3, and for a 150 mm/min type 4. After fracture, a residual burr could be observed on all specimens. The control temperatures applied in this work have no apparent effect on the fracture surface. However, type 1 could only be seen at specimens welded at the lowest feed rate with no heating. Moreover, at a feed rate of 50 mm/min with a control temperature of 60 °C ($R \rightarrow A$), type 2 could be
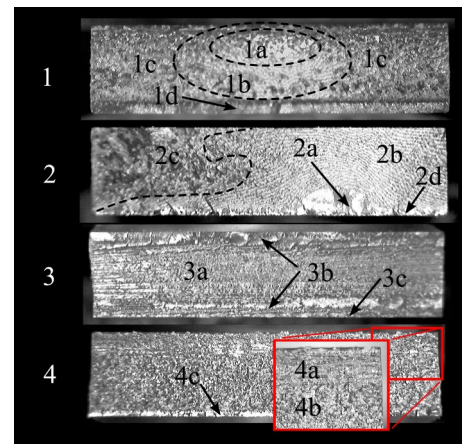

Fig. 9 Four different types of fracture surfaces (**1**,**2**,**3**,**4**) were identified. Each fracture type features characteristic regions. (**1**) 1a Mirror region, 1b Mist region, 1c Hackle region, 1d Burr. The whole fracture surface features small deepenings. (**2**) 2a Mirror region, 2b Mist region, 2c Hackle region, 2d Burr. (**3**) 3a Region with deep linear grooves, 3b Region with very flat grooves, 3c Burr. (**4**) 4a Hackle region, 4b Region with deep linear grooves, 4c Burr. The whole fracture surface is rough and features many small deepenings

observed when breaking on the AS, whereas type 3 could be identified when breaking on the RS. In contrast, only type 2 was found when the flow direction was changed. Therefore, it is assumed that the fracture surfaces could be influenced by applying further control temperature conditions. In order to get a better understanding of the failure mechanisms, the authors propose that the correlation between the control temperature and the fracture surfaces utilizing a shoulder with different zones should be investigated (see Fig. 8).

The mirror (2) and the region with deep linear grooves (4) are always on the side where the stationary shoulder was set on the specimen. Consequently, there is principally a different bonding strength on the top and bottom independent of the process parameters of this work. This is assumed to be due to a relevant temperature gradient over the thickness through the cooling from only one side. This phenomenon has to be further investigated by measuring the temperatures on the backing plate and by introducing a backing plate with a fluid temperature control.

The microstructure of the base material and the weld seam was investigated using Fourier transform infrared spectroscopy on the specimens welded at feed rates of 50 mm/min and 150 mm/min. The band structures were compared to the reference spectrum of Haken et al. [31]. It was found that the welded material uniformly differs from the base material independently of the temperature control approach and the feed rate: the material of the weld seams shows a different band structure within the CH stretching region (methyl and methylene groups) compared to the base material. Notably, no new transmission bands

appeared in the spectra of the welded material compared to the base material. Accordingly, it is assumed that there is no thermal degradation of PMMA during the welding process but a rearrangement of the molecular structure [32]. Consequently, this technology is well suited to avoiding thermal degradation of PMMA during FSW.

4 Conclusion

This paper presents a stationary shoulder with a fluid temperature control that is also capable of cooling the process. The transverse flow enabled asymmetric temperature control conditions and allows the heat transport between AS and RS to be influenced. After the explanation of the design concept, the effect of the feed rate, water flow direction, and control temperature was examined. By assessing the tensile strengths, the cross sections, the fracture surfaces, and the microstructure, the following conclusions were drawn:

- The joint consists of two bonds: one on the AS and one on the RS. The strength of these bonds is more crucial for the joint efficiency than the number of bubbles in the weld seam.
- It was shown that the ideal control temperature is different for both bonds. This optimal control temperature depends on the feed rate.
- The material transport was not influenced significantly with this asymmetric temperature control approach.
- The tensile strength was increased by cooling the process at 100 mm/min. To improve the effectiveness of the temperature control, a new shoulder with independent temperature-controlled areas is necessary.
- Heat transport from the warmer AS to the colder RS was established using the transverse flow, which improved the strength.
- The optical appearance of the fracture surface decidedly depends on the feed rate.
- The chemical microstructure of the welded specimens uniformly differs from the one of the base material independently of the temperature control approach and the feedrate.

Declarations

References

1. Mishra RS, Ma Z (2005) Friction stir welding and processing. Mater Sci Eng R Rep 50(1–2):1–78
2. Colligan K et al (1999) Material flow behavior during friction stir welding of aluminum. Welding Journal-New York- 78:229–s
3. Thomas WM, Nicholas ED, Needham JC, Murch MG, Templesmith P, Dawes CJ (G.B. Patent Application No.9125978, Dec. 1991) Improvements relating to friction welding
4. Moharami A, Razaghian A, Babaei B, Ojo O, Šlapáková M (2020) Role of mg2si particles on mechanical, wear, and corrosion behaviors of friction stir welding of aa6061-t6 and al-mg2si composite. J Compos Mater 54(26):4035–4057
5. Huang Y, Meng X, Xie Y, Wan L, Lv Z, Cao J, Feng J (2018) Friction stir welding/processing of polymers and polymer matrix composites. Compos A Appl Sci Manuf 105:235–257
6. Lambiase F, Derazkola A, Simchi A (2020) Friction stir welding and friction spot stir welding processes of polymers-state of the art. Materials 13(10):2291
7. Iftikhar SH, Mourad AHI, Sheikh-Ahmad J, Almaskari F, Vincent S (2021) A comprehensive review on optimal welding conditions for friction stir welding of thermoplastic polymers and their composites. Polymers 13(8):1208
8. Pereira MA, Galvão I, Costa JD, Amaro AM, Leal RM (2022) Joining of fibre-reinforced thermoplastic polymer composites by friction stir welding-a review. Appl Sci 12(5):2744
9. Hornbogen E, Eggeler G, Werner E (2019) Werkstoffe: Aufbau und Eigenschaften von Keramik-, Metall-. Polymer-und Verbundwerkstoffen, Springer, Berlin
10. Mittermeier C, Lion A (2020) Challenges in the experimental investigation of the caloric and thermomechanical behaviour of semi-crystalline polymers: a study on the example of polyethylene terephthalate (pet). Polym Testing 81:106252
11. Nelson TW, Sorenson CD, Johns CJ (2004) Friction stir welding of polymeric materials. US Patent 6,811,632
12. Lohwasser D, Chen Z (2009) Friction stir welding: From basics to applications

13. Simões F, Rodrigues D (2014) Material flow and thermo-mechanical conditions during friction stir welding of polymers: literature review, experimental results and empirical analysis. Mater Des 59:344–351

14. Eslami S, Ramos T, Tavares PJ, Moreira P (2015) Shoulder design developments for fsw lap joints of dissimilar polymers. J Manuf Process 20:15–23

15. Nath RK, Maji P, Barma JD (2019) Development of a self-heated friction stir welding tool for welding of polypropylene sheets. J Braz Soc Mech Sci Eng 41(12):1–13

16. Vijendra B, Sharma A (2015) Induction heated tool assisted friction-stir welding (i-fsw): A novel hybrid process for joining of thermoplastics. J Manuf Process 20:234–244

17. Banjare PN, Sahlot P, Arora A (2017) An assisted heating tool design for fsw of thermoplastics. J Mater Process Technol 239:83–91

18. Ahmed H, van Tooren M, Justice J, Harik R, Kidane A, Reynolds A (2019) Investigation and development of friction stir welding process for unreinforced polyphenylene sulfide and reinforced polyetheretherketone. J Thermoplast Compos Mater 32(9):1242–1267

19. Derazkola HA, Eyvazian A, Simchi A (2020) Modeling and experimental validation of material flow during fsw of polycarbonate. Materials Today Communications 22:100796

20. Derazkola HA, Simchi A (2018) Experimental and thermomechanical analysis of the effect of tool pin profile on the friction stir welding of poly (methyl methacrylate) sheets. J Manuf Process 34:412–423

21. Elyasi M, Derazkola HA (2018) Experimental and thermomechanical study on fsw of pmma polymer t-joint. Int J Adv Manuf Technol 97(1):1445–1456

22. Eslami S, Miranda JF, Mourão L, Tavares PJ, Moreira P (2018) Polyethylene friction stir welding parameter optimization and temperature characterization. Int J Adv Manuf Technol 99(1):127–136

23. Adibeig MR, Hassanifard S, Vakili-Tahami F, Hattel JH (2018) Experimental investigation of tensile strength of friction stir welded butt joints on pmma. Mater Today Commun 17:238–245

24. Mendes N, Neto P, Simão M, Loureiro A, Pires J (2016) A novel friction stir welding robotic platform: welding polymeric materials. Int J Adv Manuf Technol 85(1):37–46

25. Moochani A, Omidvar H, Ghaffarian SR, Goushegir SM (2019) Friction stir welding of thermoplastics with a new heat-assisted tool design: mechanical properties and microstructure. Welding in the World 63(1):181–190

26. Rezaee Hajideh M, Farahani M, Khanbeigi MA (2017) A hybrid thermal assisted friction stir welding approach for pmma sheets. Journal of Modern Processes in Manufacturing and Production 6(2):51–60

27. Bagheri A, Azdast T, Doniavi A (2013) An experimental study on mechanical properties of friction stir welded abs sheets. Mater Des 43:402–409

28. Thomas W, Staines G, Norris I, Frias R (2002) Friction stir welding-tools and developments

29. Plastics - determination of tensile properties. Standard, DIN Deutsches Institut für Normung e. V (March 2000)

30. Jiao D, Qu RT, Zhang ZF (2015) Macroscopic bifurcation and fracture mechanism of polymethyl methacrylate. Adv Eng Mater 17(10):1454–1464

31. Haken J, Werner R (1971) Infrared spectrum of polymethyl acrylate. Br Polym J 3(6):263–265

32. Holland B, Hay JN (2001) The kinetics and mechanisms of the thermal degradation of poly (methyl methacrylate) studied by thermal analysis-fourier transform infrared spectroscopy. Polymer 42(11):4825–4835